Infrastructure Inventory Compilation Using Single High Resolution Satellite Images

Pooya Sarabandi[1], BeverleyAdams[2], Anne S. Kiremidjian[3] Ronald T. Eguchi[4]
[1]Department of Civil and Environmental Engineering, Stanford University, USA. psarabandi@stanford.edu
[2]ImageCat. Inc., London, UK, bja@imagecatinc.com
[3]Department of Civil and Environmental Engineering, Stanford University, USA. ask@stanford.edu
[4]ImageCat. Inc., Long Beach, CA, USA, rte@imagecatinc.com

ABSTRACT

This paper introduces a methodological approach for rapidly obtaining spatial and structural information from a single high-resolution satellite image, using rational polynomial coefficients (RPCs) as a camera replacement model. Geometric information defining the sensor's orientation is used in conjunction with the RPC projection model to generate an accurate digital elevation model (DEM). This paper describes how the location (longitude and latitude) and height of individual structures are extracted by measuring the image coordinates for the corner of a building at ground level and its corresponding roof-point coordinates, and using the relationship between image-space and object-space together with the sensor's orientation. The paper proceeds to describe the implementation of this algorithm in the software package MIHEA (Mono-Image Height Extraction Algorithm), and presents the validation results for a QuickBird image of London using LiDAR coverage and independently derived survey data.

INTRODUCTION

Recent advances in high-resolution satellite imaging are extending the application of commercial images - such as those acquired by IKONOS, QuickBird and SPOT5 - to accurate 3D building modeling and geospatial information extraction. To support real-time calculations and provide an easy-to-use sensor model, many commercial high-resolution satellite image providers use Rational Function Model (RFM) as a replacement for their rigorous (physical) sensor model. RFM is a generalization of polynomial models that can be used to describe the image-to-ground relationship. RFM uses ratio of two polynomial functions to define the transformation between 3-dimensional object coordinates (latitude, longitude and height) and its corresponding 2-dimensinal image coordinates (row and column). For a given image, RFM can be expressed as:

$$r_n = \frac{f_1(\phi_n, \lambda_n, h_n)}{f_2(\phi_n, \lambda_n, h_n)}$$
$$c_n = \frac{f_3(\phi_n, \lambda_n, h_n)}{f_4(\phi_n, \lambda_n, h_n)} \quad (1)$$

where r_n and c_n are the row and column indices of pixels in the image, respectively; ϕ_n, λ_n and h_n are geodetic latitude, geodetic longitude and height above the ellipsoid, respectively.

This paper introduces a methodological approach to use a single satellite image and dynamic measurement to generate an accurate digital elevation model (DEM). In dynamic measurement mode, a pair of pixels - in the image- is selected such that they represent the corner of a building at ground level and its corresponding roof-point.

METHODOLOGY

The Rational Function Model

Most of the commercial high-resolution sensors (i.e. IKONOS and QuickBird) use cubic RFM as a replacement for their camera models. The ratio of first-order terms in RFM usually compensates for distortions caused by optical projection, second-order terms can be used to correct for earth curvature, atmospheric refraction and lens distortion while third-order terms can model other unknown distortions [1].

Polynomials f_i (i=1,2,3,4) have the general form of:

$$f = \sum_{i=0}^{3}\sum_{j=0}^{3}\sum_{k=0}^{3} a_{ijk}\phi^i\lambda^j h^k \qquad (2)$$

which can be expressed as:

$$\begin{aligned} f = {} & a_1 + a_2\lambda + a_3\phi + a_4 h + a_5\lambda\phi + a_6\lambda h + a_7\phi h + a_8\lambda^2 + a_9\phi^2 + a_{10}h^2 + a_{11}\phi\lambda h \\ & + a_{12}\lambda^3 + a_{13}\lambda\phi^2 + a_{14}\lambda h^2 + a_{15}\lambda^2\phi + a_{16}\phi^3 + a_{17}\phi h^2 + a_{18}\lambda^2 h + a_{19}\phi^2 h + a_{20}h^3 \end{aligned}$$

To determine longitude, latitude and height of a structure, one needs to measure image coordinates for corner of a building at ground level and its corresponding roof-point coordinates. For each conjugate pair obtained in this dynamic measurement, the following set of equations is obtained:

$$r_{ground} = \frac{f_1(\phi,\lambda,h_1)}{f_2(\phi,\lambda,h_1)}\ , c_{ground} = \frac{f_3(\phi,\lambda,h_1)}{f_4(\phi,\lambda,h_1)}\ , r_{roof} = \frac{f_1(\phi,\lambda,h_2)}{f_2(\phi,\lambda,h_2)}\ , c_{roof} = \frac{f_3(\phi,\lambda,h_2)}{f_4(\phi,\lambda,h_2)} \qquad (3)$$

where r_{ground}, c_{ground}, r_{roof} and c_{roof} are the measured (normalized) image coordinates of a ground-point and its corresponding roof-point on the image (conjugate pair), respectively; ϕ, λ, h_1 and h_2 are the unknown (normalized) object space coordinates.

Image Acquisition Geometry and Height Metrology

Approximate image acquisition geometry and satellite orientation can be described by sensor's elevation and azimuth angles. Sensor's elevation angle is the angle form the horizon up to the satellite [2]. The projection of sensor's line of sight to the area-of-interest (AOI) onto the horizontal plane measured clockwise defines the sensor's azimuth [2] as shown in Figures 1 and 2.

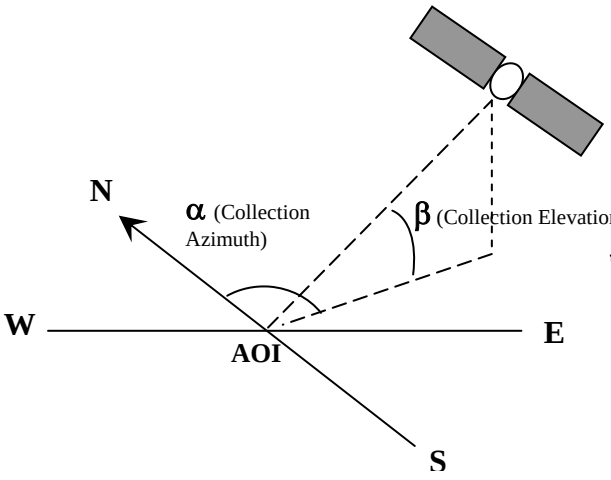

Figure 1. Image Acquisition Geometry

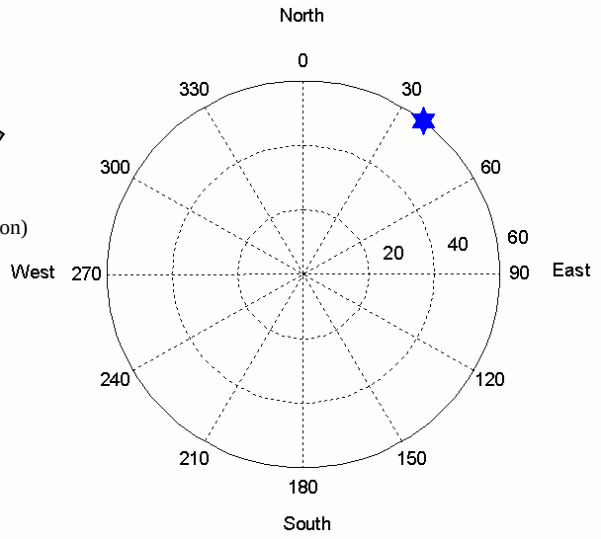

Figure 2. Image Acquisition Geometry in Polar Coordinate System (Azimuth = 37.5^{O}, Elevation = 60^{O})

By knowing a sensor's collection azimuth (β) and measuring the image coordinates for the corner of a building at ground level, (r_{ground}, c_{ground}), and its corresponding roof-point coordinates, (r_{roof} , c_{roof}), it is possible to calculate height of a building through trigonometric relationship as described in Eq. 4 and shown in Figure 3.

$$H = \frac{H^*}{\cos(\beta)} \qquad (4)$$

$$H^* = GSD \times \sqrt{(r_{ground} - r_{roof})^2 + (c_{ground} - c_{roof})^2}$$

where *GSD* is ground sample distance at the viewing angle β. *H* is the physical height of a building and H^* is the measured height of a building on the image plane.

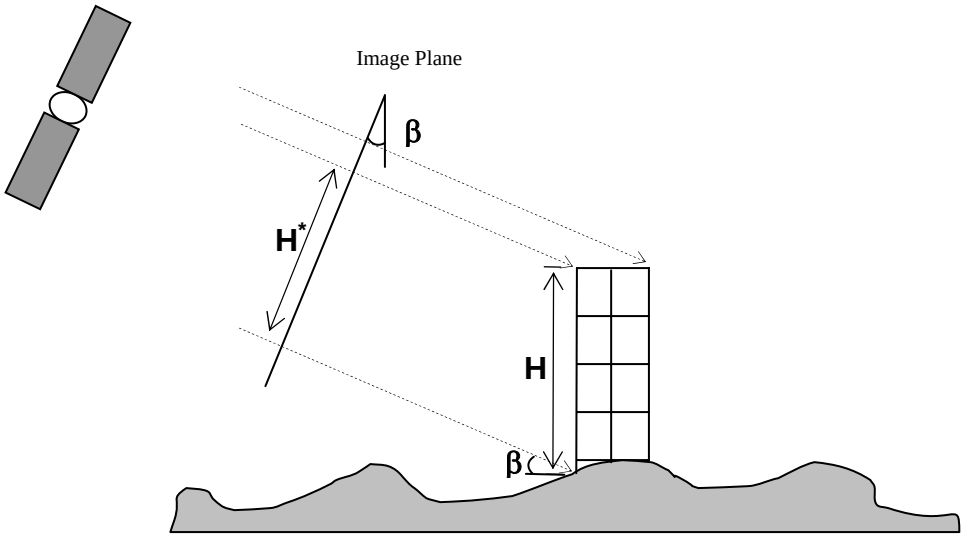

Figure 3. Relationship between real height of a building and its measured height on the image plane

3D Reconstruction Algorithm

A system of homogeneous nonlinear over-determined equations can be obtained by adding the geometric constraint for height, derived in Eq. 4, to the set of equations introduced in Eq. 3. The unknown variables are geodetic longitude, geodetic latitude, height of ground-point above the geoid and height of roof-point above the geoid, (ϕ, λ, h_1, h_2), as presented below:

$$\begin{aligned}
&\frac{f_1(\phi,\lambda,h_1)}{f_2(\phi,\lambda,h_1)} - r_g = 0 \\
&\frac{f_3(\phi,\lambda,h_1)}{f_4(\phi,\lambda,h_1)} - c_g = 0 \\
&\frac{f_1(\phi,\lambda,h_2)}{f_2(\phi,\lambda,h_2)} - r_r = 0 \\
&\frac{f_3(\phi,\lambda,h_2)}{f_4(\phi,\lambda,h_2)} - c_r = 0 \\
&(h_2 - h_1) - H = 0
\end{aligned} \tag{5}$$

The above system of nonlinear equations can be solved using the Trust-Region Dogleg Method [3] & [4]. To do this, a linear system of equations is solved to find the search direction, and the trust-region techniques [5] are used to improve the robustness of the algorithm when the starting point is far from the solution or in cases where Jacobian of design matrix (Eq. 5) is singular. The starting point $\mathbf{x_o} = (\phi^*, \lambda^*, h_1^*, h_2^*)$, used in the iterative solution of Eq. 5, can be obtained by linearizing Eq. 3 considering only the first-order terms in the numerator and denominator as expressed in Eq. 6 and Eq. 7. Singular Value Decomposition (SVD) of matrix A can be used if A becomes singular.

$$\begin{aligned}
r_g &= \frac{a_1 + a_2\lambda + a_3\phi + a_4 h_1}{b_1 + b_2\lambda + b_3\phi + b_4 h_1} + \varepsilon_1, \quad c_g = \frac{c_1 + c_2\lambda + c_3\phi + c_4 h_1}{d_1 + d_2\lambda + d_3\phi + d_4 h_1} + \varepsilon_2 \\
r_r &= \frac{a_1 + a_2\lambda + a_3\phi + a_4 h_2}{b_1 + b_2\lambda + b_3\phi + b_4 h_2} + \varepsilon_3, \quad c_r = \frac{c_1 + c_2\lambda + c_3\phi + c_4 h_2}{d_1 + d_2\lambda + d_3\phi + d_4 h_2} + \varepsilon_4
\end{aligned} \tag{6}$$

$$A \cdot \mathbf{x_o} = b \tag{7}$$

where

$$A = \begin{bmatrix} r_g b_2 - a_2 & r_g b_3 - a_3 & r_g b_4 - a_4 & 0 \\ c_g d_2 - d_2 & c_g d_3 - d_3 & c_g d_4 - d_4 & 0 \\ r_r b_2 - a_2 & r_r b_3 - a_3 & 0 & r_r b_4 - a_4 \\ c_r d_2 - d_2 & c_r d_3 - d_3 & 0 & c_r d_4 - d_4 \end{bmatrix}, \ \mathbf{x_o} = \begin{bmatrix} \phi^* \\ \lambda^* \\ h_1^* \\ h_2^* \end{bmatrix}, \ b = \begin{bmatrix} a_1 - r_g b_1 \\ c_1 - c_g d_1 \\ a_1 - r_r b_1 \\ c_1 - c_r d_1 \end{bmatrix}.$$

Measurement Error

The amount of error introduced by an operator in the process of selecting ground-points and roof-points affects the accuracy of differential-height estimation in Eq. 4 and, therefore, the overall accuracy in determining longitude, latitude and height. In this section, only the direct effect of selection-error on height is introduced. Figure 4 shows the relationship between roof-top selection-error and its corresponding error in height. Considering two independent measurements in determining the location of ground-point and roof-point, the differential-height error can be calculated as Eq. 8.

$$\sigma_H = \sqrt{2} \cdot \sec(\beta) \cdot \sigma_{Pixel} \tag{8}$$

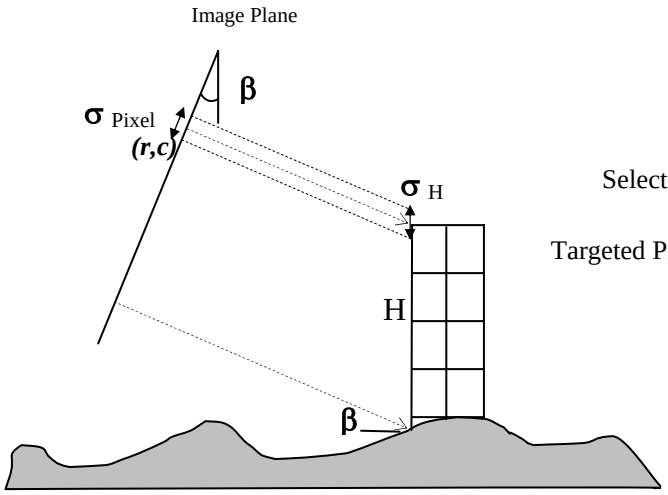

Figure 4. Height estimation error

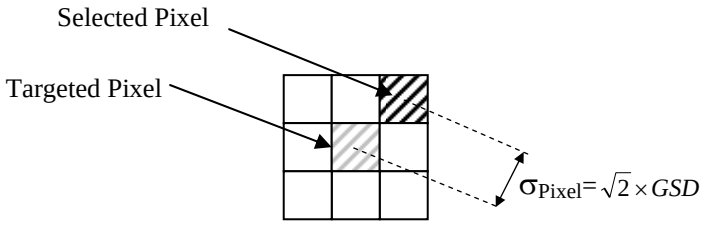

Figure 5. Pixel selection-error

Figure 5 shows the selection-error when instead of targeted pixel a neighboring pixel is selected. Table 1 summarizes the anticipated height error in IKONOS and QuickBird images for one pixel mismatch at ground-level and one pixel mismatch at roof-level.

Table 1. Maximum anticipated height error for one pixel mismatch at ground-level and roof-level

Sensor	Altitude (Km)	Off-Nadir (degree)	Collection Azimuth (β - degrees)	GSD @ off-nadir	σ_{Pixel} (m)	σ_H (m)
IKONOS	681	26	64	1.0 m	1.41	4.56
QuickBird	450	25	65	0.72 m	1.02	3.23

IMPLEMENTATION

The 3D reconstruction algorithm introduced in previous sections is implemented in the image processing package MIHEA (Mono-Image Height Extraction Algorithm). Single high-resolution satellite images (i.e. IKONOS and QuickBird) and their camera model (RFM) can be directly imported into MIHEA. MIHEA provides a graphical user interface enabling user to interactively select a ground-point and its corresponding roof-point as well as other rooftop points on a building. For each selected object (building) a set of spatial and structural attributes such as longitude, latitude, height, footprint, number of stories and total floor area of the structure are calculated. Figure 6 shows MIHEA's graphical interface as well as a 3D model created by the program. Figure 7 shows a 3D model of city of London, digitized using MIHEA.

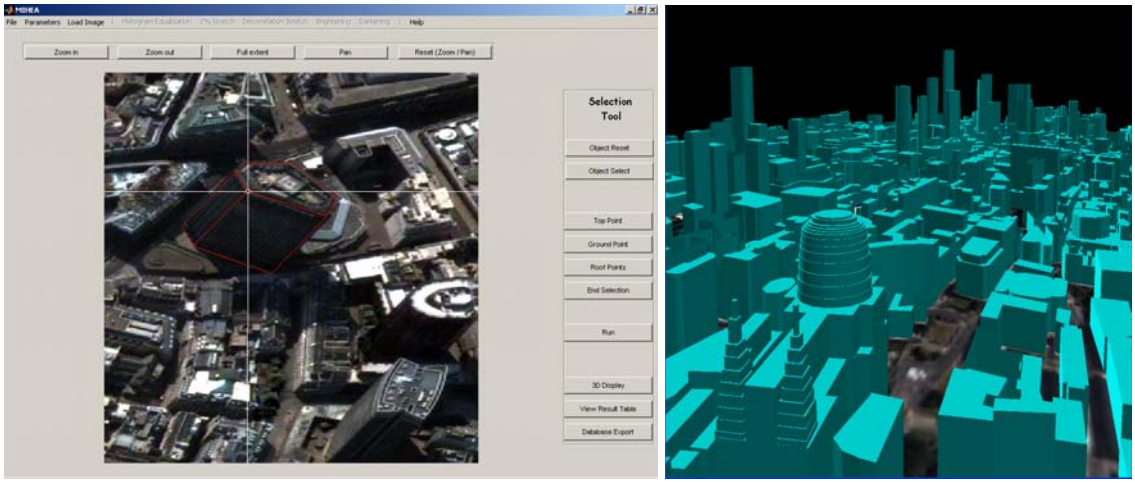

Figure 6. Mon-Image Height Extraction Algorithm (MIHEA) and 3D model of London

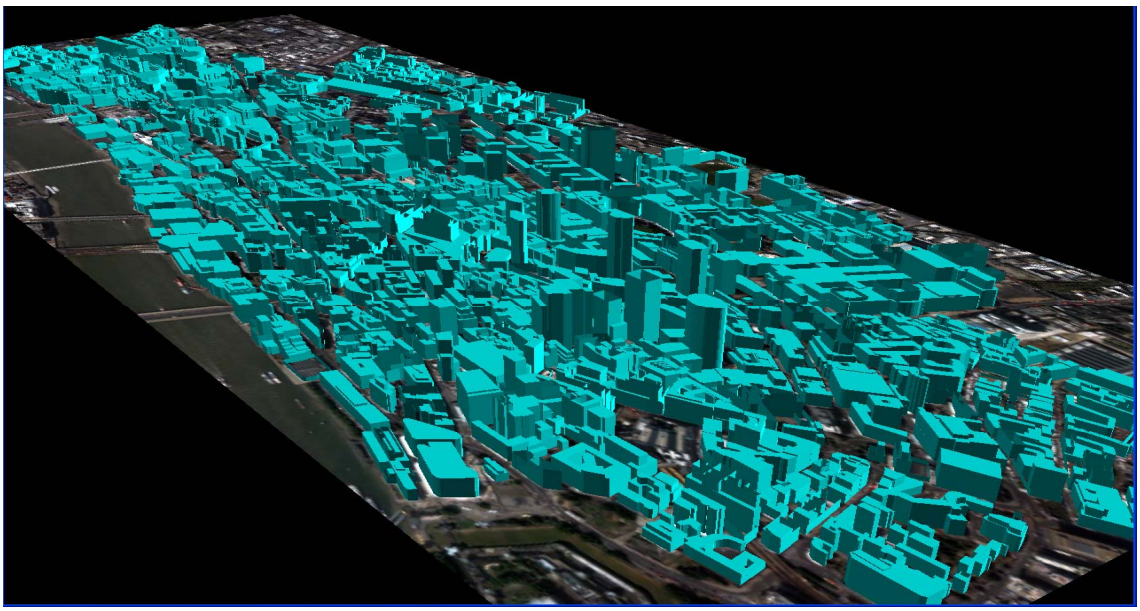

Figure 7.3D model of London created using MIHEA

RESULTS AND CALIBRATIONS

MIHEA is used to construct a 3D model of the city of London (as it can be seen in Figure 7) from a Pansharpened QuickBird image, acquired on July 28, 2002, with collection elevation angle of 65.4^{o} (off-nadir viewing angle of 24.6^{o}). The height reconstruction results are compared to the LiDAR data as well as independently derived survey data. 23 buildings are selected from generated elevation model to be used to calibrate the model. Figure 8 shows the histogram of height distribution for the selected subset of buildings. Figures 9 and 10 show linear calibration functions derived using 23 buildings from the test area. The RMS error in estimating height by MIHEA in comparison to LiDAR data is 2.67 meters whereas the RMS error in comparison to the independently derived survey data is 3.84 meters. The RMS error in estimating height in both cases is within the anticipated height error as it is shown in Table 1.

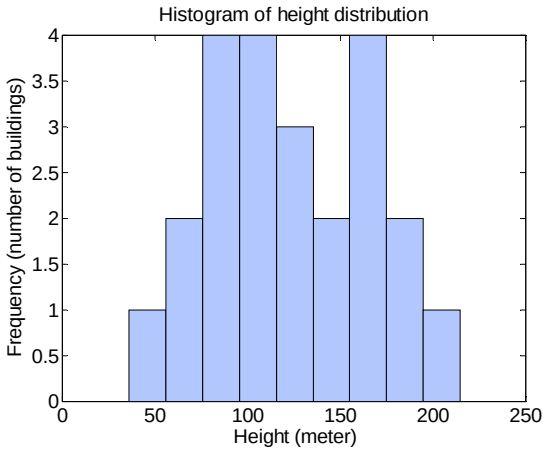

Figure 8.Histogram of height distribution for 23 buildings

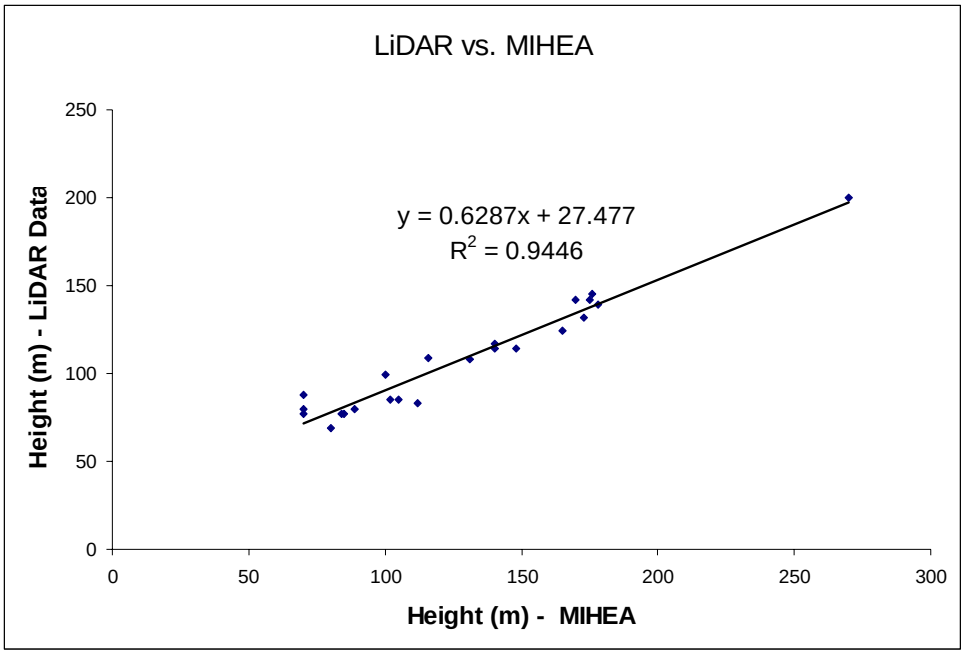

Figure 9. Model Calibration: MIHEA vs. LiDAR data.

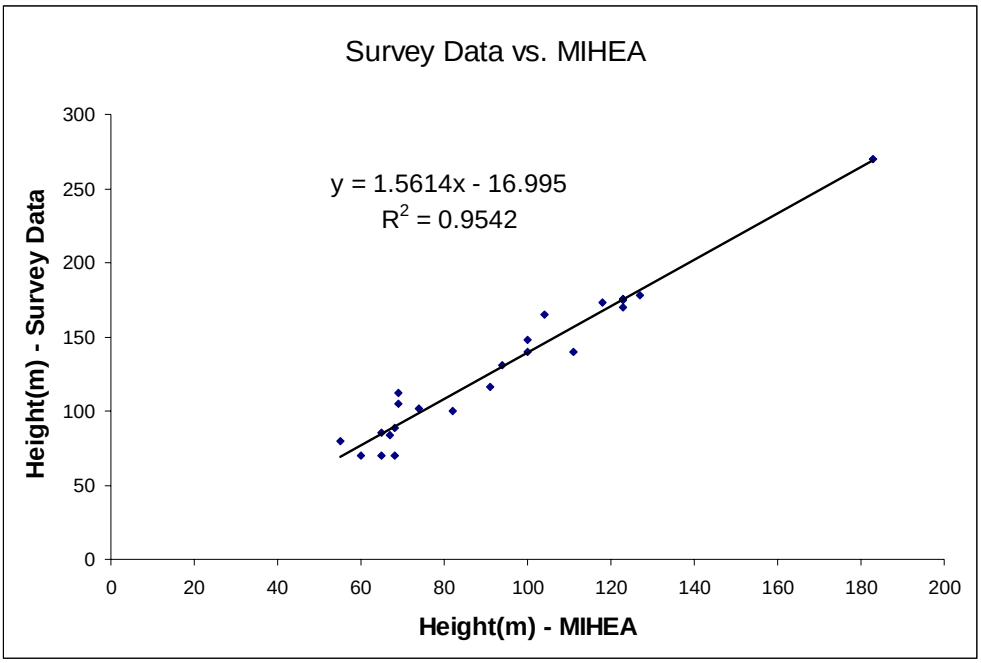

Figure 10. Model Calibration: MIHEA vs. Survey Data

ACKNOWLEDGEMENT

This research was partially supported by a grant from the UPS Foundation at Stanford University and by ImageCat, Inc. We gratefully acknowledge their support. Authors would like to thank Mike Eguchi from ImageCat Inc. for his help in digitizing buildings.

REFERENCES

[1] Grodecki, J., Dial G. and Lutes J., (2004), "Mathematical Model for 3D Feature Extraction from Multiple Satellite Images Described by RPCs," *ASPRS conference proceedings*, Denver Colorado.

[2] Grodecki, J., Dial G. and Lutes J., 2004, "Error Propagation in Block Adjustment of High-Resolution Satellite Images," *ASPRS conference proceedings,* May 2004, Anchorage, Alaska

[3] Powell, M.J.D., "A *Fast Algorithm for Nonlinearly Constrained Optimization Calculations*," Numerical Analysis, G.A.Watson ed., Lecture Notes in Mathematics, Springer Verlag, Vol. 630, 1978.

[4] Powell, M.J.D., "*A Fortran Subroutine for Solving Systems of Nonlinear Algebraic Equations*," Numerical Methods for Nonlinear Algebraic Equations, (P. Rabinowitz, ed.), Ch.7, 1970.

[5] Moré, J.J. and D.C. Sorensen, "Computing a Trust Region Step," *SIAM Journal on Scientific and Statistical Computing,* Vol. 3, pp 553-572, 1983.